EVIDENCE OF IRRADIATION IN INTERPLANETARY SPACE IN MINERALS FROM AN ULTRACARBONACEOUS ANTARCTIC MICROMETEORITE (UCAMM). C. Engrand[1], E. Charon[2], H. Leroux[3], M. Marinova[4], J. Duprat[1], E. Dartois[5], B. Guérin[1], J. Rojas[1], L. Delauche[1], M. Godard[1], D. Troadec[6]. [1]Univ. Paris-Saclay, CNRS, IJCLab, 91405 Orsay Campus, France (cecile.engrand@u-psud.fr), [2]NIMBE, CEA, CNRS, Univ. Paris-Saclay, CEA Saclay 91191 Gif-sur-Yvette France. [3]UMET CNRS/Univ. Lille, 59650 Villeneuve d'Ascq, France. [4]Chevreul Institute, CNRS/Univ. Lille, 59650 Villeneuve d'Ascq, France. [5]Univ. Paris-Saclay, CNRS, ISMO, 91400 Orsay, France. [6]IEMN CNRS/Univ. Lille, 59652 Villeneuve d'Ascq, France.

Introduction: Ultracarbonaceous Antarctic Micrometeorites (UCAMMs) are dominated by N-rich polyaromatic organic matter exhibiting large D enrichments [1-5]. The high abundance of organic matter exhibiting large D enrichment suggests a cometary origin for UCAMMs [1-3]. Three kinds of organic matter are identified in UCAMMs, with different nitrogen abundances and highly variable concentrations of small (typically 30-500 nanometer) mineral aggregates embedded in the organic matter [5-8]. We focus here on a mineral assemblage embedded in one UCAMM that exhibits evidence of ion irradiation, to get insight on the formation and evolution of this cometary particle.

Sample and methods: A fragment of UCAMM DC06-06-43 (hereafter DC06-43) was carbon coated, observed by SEM/EDX, and a 100 nm thick FIB section of this fragment was made at IEMN Lille. The size of the initial UCAMM before fragmentation was ~ 25 x 30 µm. After STXM-XANES analysis, the mineralogy of the sample was investigated by TEM at UMET Lille using a FEI Tecnai G2 20 at 200 kV and FEI TITAN Themis at 300 kV [9].

Results : TEM examination reveals a large assemblage of crystalline minerals at the center of the DC06-43 UCAMM fragment, surrounded by organic matter (**Figure 1**) [9]. The assemblage consists of µm- to sub-µm sized Mg-rich pyroxenes, a large "triskell"-shaped Fe-sulfide, a few Mg-rich olivines, and minor Si-Al-Ca-rich amorphous pockets and Fe-Ni metal. About 28 crystalline pyroxenes are identified whereas only 5 olivine crystals are observed in the section. GEMS are present embedded in the organic matter, close to the crystalline assemblage.

We identified irradiation features (rims and tracks) in pyroxene grains. No rims or tracks were found in olivine. We observed irradiated rims around six pyroxenes at the top of the section (**Figure 1,** light blue labels). One pyroxene shows a continuous irradiated rim (**Figure 2** top). Rim thicknesses range from 20 to 100 nm, with an average of 60 ± 20 nm (1σ) (**Figure 2** bottom). Fe-rich deposits are occasionally found on top of irradiated rims. EDX mappings and profiles show that the rims are strongly depleted in Mg (**Figure 3**). The average track density in pyroxene grains measured over an area of 4.5×10^{-8} cm^2 is 1.3×10^{10} cm^{-2} with one value at 3.8×10^9 cm^{-2}, the other values ranging from 9.5×10^9 to 3.2×10^{10} cm^{-2} (**Figure 4**). Irradiation track lengths range from 10 nm to ~ 1 µm (average 166 ± 113 nm, 1σ), for the ~ 100 nm thick FIB section. There is no preferred orientation of the tracks. The pyroxene grains located at the upper edge of the assemblage (labeled in light blue in **Figure 1**) contain both rims and tracks. Some tracks are observed across two adjacent pyroxene crystals.

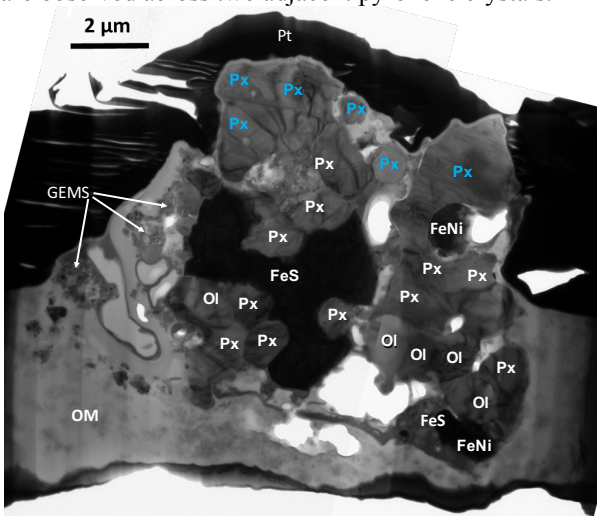

Figure 1: TEM micrograph (in bright field mode) of the FIB section of DC06-43. The mineralogy and nature of the components are annotated on the image (OM – organic matter, Px – pyroxene, Ol – olivine, FeS – iron sulfide, FeNi – iron-nickel metal, GEMS – Glass Embedded with Metals and Sulfides, Pt – platinum used for the sample preparation).

Discussion: Calculations have been carried out using the Stopping and Range of Ions in Matter (SRIM) software [10] to estimate the range of damage caused by ion irradiation as a function of energy. The range of rim thicknesses from 20 to 100 nm is compatible with irradiation with energies ranging from 1 to 5 keV/nucleon by H to Fe ions. The track lengths (up to ~ 1 µm) require irradiation at much higher energy (>10 keV/nucleon). The rims are likely produced by low energy Solar Wind (SW) whereas the tracks result from irradiation by more energetic Solar energetic particles (SEP). As observed in lunar samples and IDPs [e.g. 11, 12], the irradiated rims are strongly depleted in Mg, likely due to a selective sputtering of Mg relative to Si. The presence of a continuous rim around the pyroxene in **Figure 2** suggests a 4π irradiation of this mineral by SW before incorporation in the UCAMM.

The occurrence of tracks across pyroxene grain boundaries shows that the irradiation happened after the

formation of the mineral aggregate. An igneous origin for this aggregate is suggested by the presence of small interstitial glassy pockets rich in Si-Al-Ca that are reminiscent of a mesostasis.

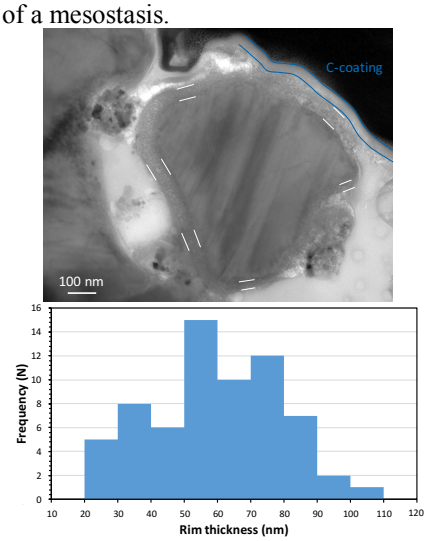

Figure 2: (top) Example of pyroxene exhibiting a continuous irradiated rim (white marks). (bottom) Histogram of irradiated rim thicknesses measured on five pyroxenes.

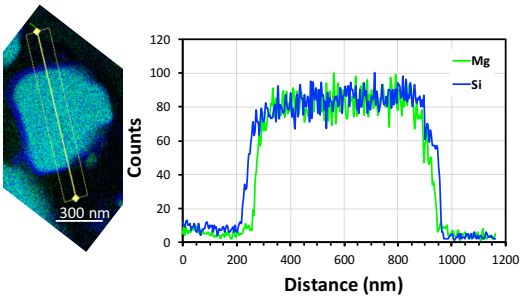

Figure 3: EDX profile through the mineral shown in Figure 2 top. (Left) EDX map showing the repartition of Si (blue) and Mg (green). (Right) intensity of Mg and Si across the mineral. The Mg depletion in the rim is very clear on both sides of the profile.

The current track production rate at 1 AU determined by Berger & Keller [13] is (4.1 ± 1.2) x 10^4 tracks.cm^{-2}.yr^{-1} (2π exposure). In these conditions, the average track concentration in DC06-43 would correspond to an exposure duration of (3.2 ± 0.9) x 10^5 years at 1 AU in current Sun conditions, or for up to ~ 3 Myrs at 3 AU, assuming that the solar energetic particle flux decays as a function of r^{-2} (r being the distance from the Sun) [14]. In the case of pre-accretionary exposure, the required irradiation time may be shorter than previously calculated if the irradiation happened close to the more active young Sun. In that case, the transport mechanism of these minerals to the UCAMM forming region (expected to be beyond the nitrogen snow line [2]) should be at low temperature (< 500ºC) in order to preserve the irradiation tracks.

Irradiation tracks are also produced during the interplanetary journey of the dust particles. For a 30 µm particle like DC06-43 travelling from a distance of 5 UA (from a JFC for instance), the calculated track production assuming a pure Poynting-Robertson (PR) drag would yield a concentration of ~ 2 x 10^9 tracks.cm^{-2}. An origin at 50 AU only increases the concentration to ~ 3 x 10^9 tracks.cm^{-2}, still a factor of 4 to 5 lower than the average value measured in DC06-43. This is comparable to the situation observed for 10 µm IDPs, for which an additional source of irradiation tracks is required [15].

We have shown that the precursor of the organic matter of UCAMMs could be produced by irradiation of N- and CH_4-rich ices by high energy galactic cosmic rays (GCR) at the surface of small bodies in the outer regions of the protoplanetary disk [2, 16]. If the minerals were embedded under a few meters of these ices, GCR may also have contributed to the track production. Another explanation could also invoke a more complicated orbital evolution than simply governed by pure PR-drag. For instance, mean motion resonances with giant planets during the journey of UCAMMs toward the Earth could possibly trap the particles and increase the exposure duration of UCAMM to the interplanetary radiative environment.

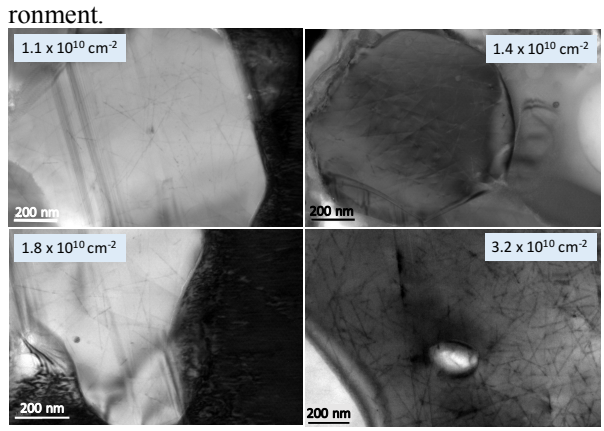

Figure 4: Selected TEM micrographs of pyroxenes showing irradiation tracks, with their respective track concentrations given in insets.

Acknowledgments: Funding from CNRS, PNP, CNES, LabEx P2IO, IN2P3 DIM-ACAV and ANR (COMETOR), and logistic support from IPEV-PNRA in Antarctica are acknowledged.

References: [1] Duprat J. et al. (2010) *Science 328*, 742-745. [2] Dartois E. et al. (2013) *Icarus 224*, 243-252. [3] Dartois E. et al. (2018) *A&A 609*, A65. [4] Nakamura T. et al. (2005) *MAPS 40 Suppl.*, #5046. [5] Yabuta H. et al. (2017) *GCA 214*, 172-190. [6] Dobrică E. et al. (2012) *GCA 76*, 68-82. [7] Engrand C. et al. (2018) *LPSC 49*, #2015. [8] Guerin B. et al. (2020) *LPSC 51*, in press. [9] Charon E. et al. (2017) *LPSC 48*, #2085. [10] Ziegler J.F., *SRIM - the Stopping and Range of Ions in Matter*. 2013. [11] Bradley J.P. (1994) *Science 265*, 925-929. [12] Keller L.P. and McKay D.S. (1997) *GCA 61*, 2331-2341. [13] Berger E.L. and Keller L.P. (2015) *LPSC 46*, 1543. [14] Hamilton D.C. et al. (1990) in *International Cosmic Ray Conference 5* 237. [15] Keller L.P. and Flynn G.J. (2019) *LPSC*. [16] Augé B. et al. (2016) *A&A 592*, A99.